Available online at www.sciencedirect.com
ScienceDirect
Journal of Catalysis 254 (2008) 285–295
JOURNAL OF CATALYSIS
www.elsevier.com/locate/jcat

A quantitative determination of reaction mechanisms from density functional theory calculations: Fischer–Tropsch synthesis on flat and stepped cobalt surfaces

Jun Cheng [a], Xue-Qing Gong [a], P. Hu [a,*], C. Martin Lok [b], Peter Ellis [c], Sam French [c]

[a] *School of Chemistry and Chemical Engineering, The Queen's University of Belfast, Belfast, BT9 5AG, UK*
[b] *Johnson Matthey Technology Centre, Billingham Cleveland, TS23 1LB, UK*
[c] *Johnson Matthey Technology Centre, Reading, RG4 9NH, UK*

Received 10 September 2007; revised 23 December 2007; accepted 3 January 2008

Available online 11 February 2008

Abstract

We systematically investigated the mechanism of the $C_1 + C_1$ coupling reactions using density functional theory. The activation energies of $C_1 + C_1$ coupling and carbon hydrogenation reactions on both flat and stepped surfaces were calculated and analyzed. Moreover, the coverages of adsorbed C_1 species were estimated, and the reaction rates of all possible $C_1 + C_1$ coupling pathways were quantitatively evaluated. The results suggest that the reactions of $CH_2 + CH_2$ and $CH_3 + C$ at steps are most likely to be the key $C_1 + C_1$ coupling steps in FT synthesis on Co catalysts. The reactions of $C_2 + C_1$ and $C_3 + C_1$ coupling also were studied; the results demonstrate that in addition to the pathways of $RCH + CH_2$ and $RCH_2 + C$, the coupling of $RC + C$ and $RC + CH$ also may contribute to the chain growth after C_1.
© 2008 Elsevier Inc. All rights reserved.

Keywords: Fischer–Tropsch; DFT; Co; Mechanism; C–C coupling

1. Introduction

Fischer–Tropsch (FT) synthesis [1–7] is of paramount importance in the utilization of natural resources, such as natural gas and coal. It has attracted wide interest [8–17] since it was discovered around 80 years ago [18]. In particular, it has attracted much attention in the past few years due to the unremitting rising price of crude oil. Generally speaking, FT synthesis is a process for transforming CO and H_2, which can be obtained by treating natural gas, into long-chain hydrocarbons. It involves a complex reaction scheme comprising many surface intermediates and elementary reaction steps. The main reaction mechanism of the process (i.e., the C + C coupling reactions that are responsible for chain growth) remains a topic of serious debate. Three mechanisms have been proposed. First, the carbene mechanism suggested by Fischer and Tropsch [1] themselves implies that the C + C coupling is achieved through polymerization of CH_2 intermediates on the surface. Second, Anderson and Emmett [19] proposed the hydoxy-carbene mechanism in which the C + C coupling progresses from dimerization between adsorbed hydroxyl methylene intermediates. Third, Pichler and Schulz [20] suggested the CO-insertion mechanism, in which C + C coupling occurs through insertion of CO into adsorbed alkyl intermediates.

A breakthrough in studying FT synthesis mechanism was made by Brady and Pettit [21,22], who for the first time demonstrated the importance of adsorbed CH_2 species on the catalyst surface, which largely supports the carbene mechanism. They obtained a product distribution similar to that of FT product through reactions between diazomethane and hydrogen over Co, Fe, and Ru, the main FT catalysts. In addition, van Barneveld and Ponec [23] also discovered that CH_xCl_{4-x} hydrogenation in the presence of FT catalysts can produce methane and long-chain hydrocarbons. All of these non-oxygen experiments imply that C + C coupling can occur in the absence of oxygen. The results suggest that the two other mechanisms, both involving oxygen, may not be major ones under typical

* Corresponding author. Fax: +44 (0) 28 9097 4687.
E-mail address: p.hu@qub.ac.uk (P. Hu).

0021-9517/$ – see front matter © 2008 Elsevier Inc. All rights reserved.
doi:10.1016/j.jcat.2008.01.009

reaction conditions. Meanwhile, with the development of spectroscopy in heterogeneous catalysis, CH_x ($x = 0$–3) surface species were detected in situ and ex situ on many metal surfaces [24–28]; therefore, the carbene mechanism seems more plausible. It is now widely accepted that FT synthesis starts with CO and H_2 dissociative adsorption, followed by hydrogenation processes to generate CH_x ($x = 1$–3) intermediates and C + C coupling reactions to form high-weight hydrocarbons.

In the traditional carbene mechanism, the CH_2 group is considered the monomer and a CH_3-like intermediate (e.g., CH_2CH_3) is considered the growing chain. However, density functional theory (DFT) calculations have demonstrated that the CH_2 species is the C_1 species with the lowest stability on metal surfaces (Co and Ru) [29,30], and that $CH_2 + CH_2R$ (R = H or alkyl) has high barriers [31]. This indicates that the chain growth pathway of the carbene mechanism may be difficult to achieve. Accordingly, some other C + C coupling mechanisms have been suggested. Ciobîcă and van Santen studied CH_x adsorption and the chain growth mechanism in FT synthesis over flat Ru(0001) using DFT calculations [32–34] and reported that CH is the most stable C_1 species. This suggests that CH is most likely the monomer in the chain growth process. Their results are consistent with the experimental results of Wu and Goodman [35,36]. Based on this, these authors suggested two different propagation cycles in which chain growth steps can be expressed by RCH + CH and RCH_2 + CH (R = H or alkyl). At almost the same time, Liu and Hu [31] carried out DFT calculations to investigate hydrogenation reactions and several C + C coupling reactions on both flat and stepped Ru(0001). Their results indicated that C + C coupling is favored on the stepped surface; thus, they suggested a new mechanism in which the C atom and RC group are the monomer and growing chain, respectively, and the C + RC coupling reaction occurs through the transition state, with the RC on the step edge and the C is on the terrace below.

Both theoretically and experimentally, steps have been found to play a very important role in FT synthesis [37,38]. Using DFT calculations, Gong et al. studied some elementary reactions in FT synthesis over Co(0001) [28,39] and found that CO dissociation and water formation are favored at steps, and that most surface species (e.g., CH_x [$x = 0$–3]) prefer to adsorb on the step sites. Dramatic surface restructuring on the flat Co(0001), which leads to the formation of numerous atomic steps, was observed by Wilson and de Groot under FT reaction conditions using STM [40]. These authors further determined that the fraction of all cobalt atoms in the uppermost atomic layer occupying edge sites was as high as ∼50%. For the same system, Beitel et al. investigated the adsorption of CO and coadsorption of CO with H_2 in situ by PM-RAIRS [41,42]. According to their spectroscopic results, CO attached to cobalt at steps disappeared under FT reaction conditions. These authors suggested that hydrocarbons were formed on such defect sites and blocked the adsorption of CO at these positions.

Reaction mechanisms have been hot issues in every catalytic system. Traditionally, many mechanisms were proposed based on the following qualitative understanding of a system:

1. Experimentally, one measures all possible intermediates in the system, and then, with other information, posits a plausible mechanism involving one or several key intermediates observed. A major problem in this approach is that the intermediates that can be measured experimentally are usually stable and may be spectators, whereas species that cannot be "seen" experimentally are reactive and may be the key species in the process.
2. One determines, either experimentally or theoretically, some barriers in the system, compares the different pathways based on information from the barriers, and, finally, suggests a possible mechanism. A major concern with this approach is that the barrier is not the only parameter that can affect the rate of the system; for example, varying surface coverages of adsorbates can change the rate of a process in a catalytic system according to the rate law (see Section 4).

Consequently, it is not surprising that the mechanism is a matter of intensive debate in almost all catalytic systems. This raises a fundamental question in chemistry: How can we determine the mechanism in a catalytic system with a complicated network of reactions?

In this work, we investigate the mechanism of FT synthesis on Co catalysts using DFT calculations, aiming to answer this question. The FT synthesis was chosen for two reasons. First, it is a very important reaction, being related to the central issue in this century: energy. A better understanding of the mechanism of the process should provide a foundation for improving the process. Second, it is one of the most complicated systems, and an approach developed for this system possibly may be extended to other systems. We studied all possible $C_1 + C_1$ coupling reactions on both flat and stepped Co(0001) using DFT calculations. In conjunction with the carbon hydrogenation, we analyzed the chain growth mechanism of FT reactions quantitatively.

The paper is organized as follows. In the next section, we describe our calculation method. We then present the results of calculations for the coupling reactions on both flat and stepped Co(0001). In the Discussion section, we evaluate the C_1 species coverages and all $C_1 + C_1$ coupling rates on both surface sites to characterize the C + C coupling mechanism in FT synthesis. We end with some conclusions.

2. Computational details

In this work, the SIESTA code was used with Troullier–Martins norm-conserving scalar relativistic pseudopotentials [43–45]. A double zeta-plus polarization (DZP) basis set was used. The localization radii of the basis functions were determined from an energy shift of 0.01 eV. A standard DFT supercell approach with the Perdew–Burke–Ernzerhof (PBE) form of the generalized gradient approximation (GGA) functional was implemented with a mesh cutoff of 200 Ry. Spin polarization was included in the calculations. The calculated lattice constants of the Co primary cell were 2.560, 4.140 Å (exp.: 2.507, 4.069 Å). The accuracy of calculations was evaluated by com-

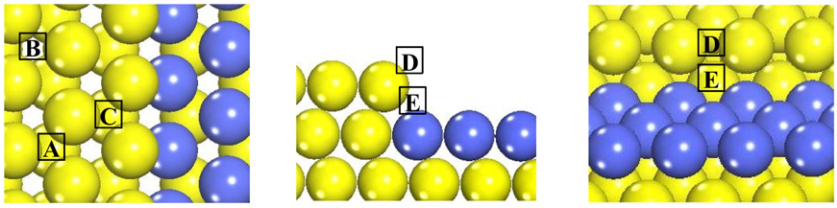

Fig. 1. The top view (left), the side view (middle) and another side view (right) of the stepped Co(0001). The Co atoms on the top terrace are in yellow, the Co atoms on the terrace below in blue. (A) The hcp site; (B) the fcc site; (C) the near-edge-hcp site; (D) the edge-bridge site; and (E) the step-corner site. This notation is used throughout the paper. (For interpretation of the references to color in this figure legend, the reader is referred to the web version of this article.)

Table 1
Comparison of the chemisorption energies of CH_x ($x = 0$–3) from SIESTA and CASTEP

Species	SIESTA			CASTEP		
	$E_{ad,f}$	$E_{ad,s}$	ΔE_{ad}	$E_{ad,f}$	$E_{ad,s}$	ΔE_{ad}
C	−6.54	−7.32	0.78	−6.62	−7.53	0.91
CH	−6.54	−6.88	0.34	−5.99	−6.33	0.34
CH_2	−3.86	−3.98	0.12	−3.85	−4.03	0.18
CH_3	−2.00	−2.21	0.21	−1.89	−2.24	0.35

Table 2
Testing results of different models of surface steps

Adsorption on lower terrace	CH_3C at step-corner site	Adsorption on upper terrace	C at hcp hollow site
2 rows removed	−5.73 eV	2 rows of upper terrace	−6.61 eV
3 rows removed	−5.73 eV	3 rows of upper terrace	−6.64 eV

paring the calculated chemisorption energies of CH_x ($x = 0$–3) with those calculated by CASTEP in our previous work. (Table 1 shows the comparison of the chemisorption energies of CH_x ($x = 0$–3) between the present work by SIESTA and our previous work by CASTEP (in Ref. [29]). $E_{ad,f}$ and $E_{ad,s}$ are chemisorption energies on the flat surface and stepped surface, respectively. ΔE_{ad} is the difference between $E_{ad,f}$ and $E_{ad,s}$. The unit is eV.)

The reactions on terraces were studied using the $p(2 \times 2)$ unit cell in most cases, and the surface Monkhorst Pack meshes of $5 \times 5 \times 1$ k-point sampling in the surface Brillouin zone was used. To avoid an interaction between the adsorbates in neighboring unit cells, some reactions on terraces were studied in $p(3 \times 2)$ unit cell, using surface Monkhorst Pack meshes of $3 \times 5 \times 1$ k-point sampling in the surface Brillouin zone. When studying the reactions at steps, the $p(4 \times 2)$ unit cell was used, and the stepped Co(0001) was modeled by removing two neighboring rows of cobalt atoms on the top layer. (To check whether our model is appropriate, we did the following two tests: (i) the adsorption of CH_3C at the step-corner site in a $p(4 \times 2)$ unit cell with two rows removed and in a $p(5 \times 2)$ unit cell with three rows removed; and (ii) the adsorption of C on the hcp hollow site on the upper terrace in a $p(4 \times 2)$ unit cell with two rows removed and in a $p(4 \times 2)$ unit cell with one row removed. The calculated adsorption energies (E_{ad}) are listed as follows in Table 2.) Surface Monkhorst Pack meshes of $3 \times 5 \times 1$ k-point sampling in the surface Brillouin zone were used on the stepped surface. To avoid an interaction between the adsorbates in neighboring unit cells, some reactions at steps were studied in the $p(4 \times 3)$ unit cell, using surface Monkhorst Pack meshes of $3 \times 4 \times 1$ k-point sampling in the surface Brillouin zone. The different sites on the surfaces are shown in Fig. 1. In the calculations, the surfaces were modeled by four layers of metal atoms; the bottom two layers of metal atoms were fixed, and the top two layers (the upper and lower terraces for the stepped surface) and the adsorbates were relaxed.

The transition states (TSs) were searched using a constrained optimisation scheme [46–48]. The distance between the reactants was constrained at an estimated value and the total energy of the system was minimized with respect to all other degrees of freedom. The TSs can be located by changing the fixed distance, and they must be confirmed based on the following two rules: (i) all forces on atoms vanish, and (ii) the total energy is a maximum along the reaction coordinate but a minimum with respect to the rest degrees of freedom.

3. Results

To gain insight into chain growth processes, we studied all of the possible coupling reactions between C_1 species on both flat and stepped Co(0001).

3.1. The $C_1 + C_1$ coupling reactions on the flat Co(0001)

In our recent work [29], we studied the adsorption of all of the C_1 species (i.e., C, CH, CH_2, and CH_3) on flat Co(0001). We found that all of these C_1 species are most stable on the hcp hollow site under moderate coverage (0.25 ML). Therefore, in the present work we took the systems with separately adsorbed C_1 species on the hcp hollow sites as the initial states (IS) of the coupling reactions.

We located the TSs of the following coupling reactions: C + C, C + CH, C + CH_2, C + CH_3, CH + CH, CH + CH_2, CH + CH_3, CH_2 + CH_2, and CH_2 + CH_3. Fig. 2 illustrates the structures of the TSs, and Table 3 lists the distances between the two C atoms in the TSs. The figure and table clearly show some general trends in the TS configurations:

1. In the TSs of the reaction between the C atom and other C_1 species, the C atom is always sitting on the hcp hollow site, which is the most stable C adsorption site. C, CH, and CH_2 that approach the C atom are activated to the bridge site in

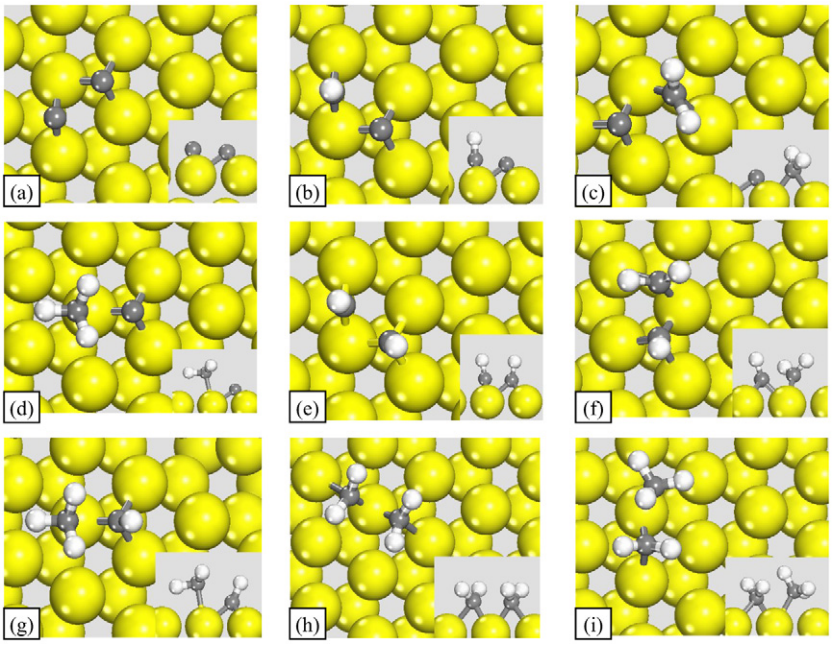

Fig. 2. Top view and side view (inserted) of the calculated TS structures of $C_1 + C_1$ coupling reactions on the flat Co(0001). (a) C + C; (b) C + CH; (c) C + CH_2; (d) C + CH_3; (e) CH + CH; (f) CH + CH_2; (g) CH + CH_3; (h) CH_2 + CH_2; (i) CH_2 + CH_3. The small ball in grey is C and the small ball in white is H. This notation is used throughout this paper.

Table 3
The barriers of the $C_1 + C_1$ coupling reactions and the C–C distances at the TSs on the flat and stepped Co(0001)

Pathway	C + C		C + CH		C + CH_2		C + CH_3	
Site	Flat	Step	Flat	Step	Flat	Step	Flat	Step
Barrier (eV)	1.22	2.43	0.91	1.96	0.74	1.34	0.94	1.09
Distance (Å)	2.08	2.31	2.00	2.63	2.05	2.52	2.12	1.97
Pathway	–		CH + CH		CH + CH_2		CH + CH_3	
Site	Flat	Step	Flat	Step	Flat	Step	Flat	Step
Barrier (eV)	–	–	0.86	1.76	0.76	1.32	1.05	1.55
Distance (Å)	–	–	1.93	2.27	1.94	2.26	1.94	1.91
Pathway	–		–		CH_2 + CH_2		CH_2 + CH_3	
Site	Flat	Step	Flat	Step	Flat	Step	Flat	Step
Barrier (eV)	–	–	–	–	0.70	0.22	1.11	0.73
Distance (Å)	–	–	–	–	2.13	2.16	2.03	2.01

these TSs, and the CH_3 group is activated to the nearby top site nearby.

2. In the TSs of the reactions between CH and CH, CH_2, and CH_3, the CH is also on the hcp hollow site, and the other CH and CH_2 groups are activated to the nearby bridge sites, whereas the CH_3 group is on the top site.
3. With respect to the reactions of CH_2 + CH_2 and CH_2 + CH_3, CH_2 sits on the bridge site, and the CH_3 is activated to the top site.

In general, the high-valence groups (C and CH) prefer to sit on the hcp hollow site in the TS, and the other group is activated to the bridge site except the CH_3, which is always on the top site in the TS. These results are consistent with those obtained by Michaelides and Hu [49] when studying C_1 hydrogenation.

From the total energies of the initial and transition states, we can estimate the energy barriers of these coupling reactions. The results are given in Table 3.

It should be mentioned that the structures of the TSs that we located on Co(0001) are very close to those obtained by Liu and Hu on Ru(0001) [31]. In particular, the result of the CH + CH_2 reaction obtained in the present work is similar to that obtained by van Santen et al. on Ru(0001) [33] and that obtained by Neurock et al. on Co(0001) and Ru(0001) [50]. For example, Neurock et al. reported a distance of 1.899 Å between the two C atoms in the TS of CH + CH_2 coupling on Co(0001) and a barrier of around 0.8 eV; the corresponding values in the present work are 1.94 Å and 0.76 eV, respectively (Table 3).

3.2. The $C_1 + C_1$ coupling reactions on the stepped Co(0001)

In recent work [29], we calculated the adsorption of different C_1 species on the stepped Co(0001) and found that C and CH had the highest adsorption energies on the step-corner site, whereas the edge-bridge site was favored by CH_2 and CH_3. Moreover, the adsorption energies generally were much higher on the stepped Co(0001) than on the flat surface. These results indicate that the area around the step edge is preferred for C_1 adsorption and thus may be the favored place for coupling reactions to occur.

Fig. 3 illustrates the structures of the TSs of the coupling reactions on stepped Co(0001). Table 3 lists the distances between the two Cs in these TSs. The figure and table demonstrate that the TSs of C + C, C + CH, and C + CH_2 are similar; the C atom is always on the hcp hollow site near the step-corner on the lower terrace, whereas the other C_1 species sits on the edge-bridge sites above. Similarities also can be found in the TSs of

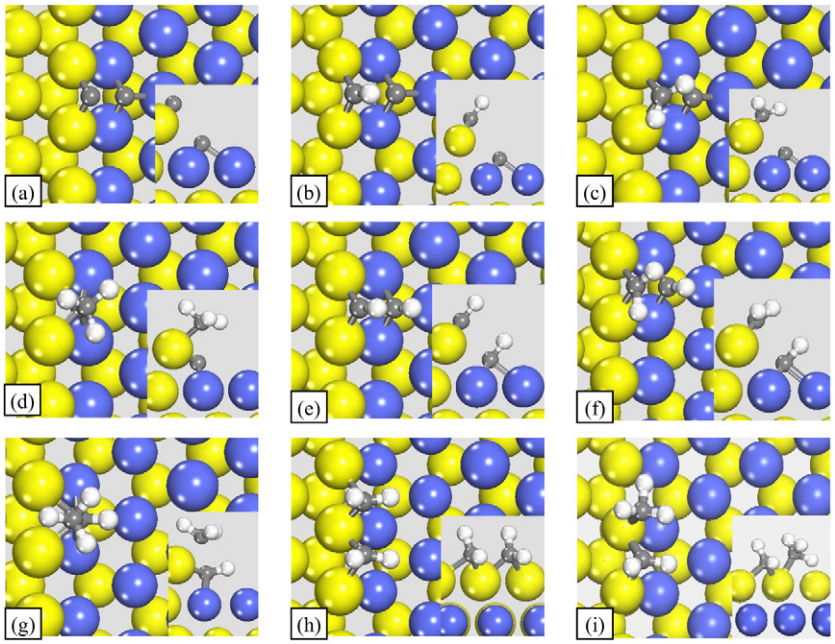

Fig. 3. Top view and side view (inserted) of the calculated TS structures of $C_1 + C_1$ coupling reactions on the stepped Co(0001). (a) C + C; (b) C + CH; (c) C + CH_2; (d) C + CH_3; (e) CH + CH; (f) CH + CH_2; (g) CH + CH_3; (h) CH_2 + CH_2; (i) CH_2 + CH_3.

CH + CH and CH + CH_2. Moreover, the TSs of C + CH_3 and CH + CH_3 share the same type of geometry, with C or CH still on the step-corner site and the CH_3 on the off-step edge. With respect to the TSs of CH_2 + CH_2 and CH_2 + CH_3, CH_2 sits on the bridge site, and CH_3 is activated to the atop site at the step edge, consistent with those on the flat surface (Fig. 2h). It should be mentioned that the TSs of the coupling reactions on the stepped Co(0001) and those obtained by Liu and Hu on the stepped Ru(0001) [31] have similar structures. From the total energies of the ISs and TSs, we can determine the energy barriers of these coupling reactions on the stepped Co(0001), which are listed in Table 3.

Carefully examining the barriers and the distances between the reacting C atoms on the flat and stepped Co(0001) listed in Table 3, it is interesting to find that the barriers on the flat surface are smaller than those on the step sites for all the coupling reactions except $CH_2 + CH_2$ and $CH_2 + CH_3$, and the distances on the flat surface change with different coupling reactions in a rather small range (2.02–2.04 Å), whereas the variation in the distances on the step sites is quite large (e.g., up to 2.63 Å for C + CH).

4. Discussion

4.1. The $C_1 + C_1$ coupling reactions on the flat and stepped surfaces

Much experimental evidence strongly suggests that surface defects play an important role in FT reaction [40–42]. According to our previous DFT calculations [39], CO dissociation and oxygen hydrogenation—the preliminary reactions in FT synthesis—indeed occur on the step sites. But for $C_1 + C_1$ coupling reactions, if only the barriers listed in Table 3 are considered, then the flat surface generally should be preferred because of the lower barriers. However, because the C_1 species prefer to adsorb on the step sites, the stability difference between ISs on the flat surfaces and stepped surfaces must be taken into account, as discussed below.

Table 4
The adsorption energies (in eV) of the C_1 species on the flat and stepped Co(0001)

Species	$E_{ad,\,f}$	$E_{ad,s}$	ΔE_{ad}
C	−6.54	−7.32	0.78
CH	−6.54	−6.88	0.34
CH_2	−3.86	−3.98	0.12
CH_3	−2.00	−2.21	0.21

$E_{ad,\,f}$ and $E_{ad,s}$ are chemisorption energies on the flat surface and stepped surface, respectively. ΔE_{ad} is the difference between $E_{ad,\,f}$ and $E_{ad,s}$. On the flat surface, the hcp hollow site is the most stable one for all the C_1 species. On the step sites, both C atom and CH prefer to adsorb on the step-corner site, and CH_2 and CH_3 on the edge-bridge site.

Table 4 lists the adsorption energies of the C_1 species with the most stable structures on the flat and stepped Co(0001). As mentioned earlier, on the flat surface, all of the C_1 species are favored on the hcp hollow site. In addition, on the stepped surface, carbon atom (C) and methylidyne (CH) prefer to sit on the step-corner site, whereas the edge-bridge sites are favored for methylene (CH_2) and methyl (CH_3). Comparing the adsorption energies on the flat and stepped surfaces (Table 4) reveals that all of the C_1 species at steps are favored; in particular, the adsorbed carbon atom is nearly 0.8 eV more stable on the step-corner site than that on the flat hcp hollow site. In addition, hydrogen has similar stabilities on the fcc hollow site of the flat surface and on the near-edge-hcp site of steps, with both sites giving similar adsorption energies of ∼−2.78 eV.

Based on the $C_1 + C_1$ coupling barriers in Table 3 and the adsorption energy differences in Table 4, all of the possible $C_1 + C_1$ coupling pathways on both the flat and stepped surfaces can be arranged in a single energy profile, as shown in Fig. 4. For each coupling pathway, the IS on the step sites is chosen as a reference state. The corresponding data are listed in Table 5. We can clearly see that in fact, all of the TSs on the step sites are more stable than those on the flat surface, except for the $CH + CH_2$ and $CH + CH$ coupling reactions.

In other words, although the barriers with respect to their corresponding ISs on the flat surface are smaller than those on the step sites, ISs and TSs are more favored on the step sites. This raises a question: Is the barrier or IS/TS stability the key to determine where reactions occur? To answer this question, we suggest the following model:

$$A_s + *_f \rightleftharpoons A_f + *_s,$$

$$B_s + *_f \rightleftharpoons B_f + *_s,$$

$$A_s + B_s \xrightarrow{r_s} C_s,$$

$$A_f + B_f \xrightarrow{r_f} C_f,$$

where A_s and B_s are surface species adsorbed on the step sites, A_f and B_f are those adsorbed on the flat surface, and $*_s$ and $*_f$ are free surface sites on the step sites and on the flat surface, respectively. In this model, it is assumed that the species of A and B can readily diffuse on the surface and that equilibria are reached. Therefore, surface intermediate concentrations on both the sites would follow the equations:

$$\frac{\theta_{A_s}}{\theta_{A_f}} = \frac{\theta_{*_s}}{\theta_{*_f}} e^{\Delta E_{\mathrm{ad},A}/(RT)} \tag{1}$$

and

$$\frac{\theta_{B_s}}{\theta_{B_f}} = \frac{\theta_{*_s}}{\theta_{*_f}} e^{\Delta E_{\mathrm{ad},B}/(RT)}, \tag{2}$$

where $\theta_{A_f}(\theta_{B_f})$ and $\theta_{A_s}(\theta_{B_s})$ are the coverages of species A (B) on the flat and stepped surfaces, respectively, θ_{*_f} (θ_{*_s}) is the free site coverage on the flat (stepped) surface, and $\Delta E_{\mathrm{ad},A}$ ($\Delta E_{\mathrm{ad},B}$) is the energy difference between the chemisorption energy of A (B) on the flat surface, $E_{\mathrm{ad},f}$, and that on the step site, $E_{\mathrm{ad},s}$.

It is generally believed that C + C coupling is irreversible under FT reaction conditions. Thus, the forward reactions are merely considered and the reaction rates on both of the sites can be given in Arrhenius forms by

$$r_s = Ae^{-E_{a,s}/(RT)}\theta_{A_s}\theta_{B_s} \tag{3}$$

and

$$r_f = Ae^{-E_{a,f}/(RT)}\theta_{A_f}\theta_{B_f}, \tag{4}$$

where E_a is the activation energy and A is the pre-exponential factor, which is assumed to be the same on both the sites. As shown in Fig. 4, the following equations also can be obtained:

$$\Delta E_{\mathrm{IS}} = \Delta E_{\mathrm{ad},A} + \Delta E_{\mathrm{ad},B} \tag{5}$$

and

$$E_{a,f} + \Delta E_{\mathrm{IS}} = E_{a,s} + \Delta E_{\mathrm{TS}}. \tag{6}$$

Based on the foregoing equations, the ratio of r_s and r_f can be expressed as

$$\frac{r_s}{r_f} = \left(\frac{\theta_{*_s}}{\theta_{*_f}}\right)^2 e^{\Delta E_{\mathrm{TS}}/(RT)} = s^2 e^{\Delta E_{\mathrm{TS}}/(RT)}, \tag{7}$$

where

$$s = \frac{\theta_{*_s}}{\theta_{*_f}}.$$

Equation (7) implies that the ratio of reaction rates on different sites is related to (i) the ratio of free site coverage on the step sites to that on the flat surface and (ii) the difference of TS energies on the flat and stepped surfaces. It is, in fact, independent of the ISs. Generally, TSs on the step sites are relatively more stable than those on the flat surface (Fig. 4), making the steps being more favorable for reactions. On the other hand, free site

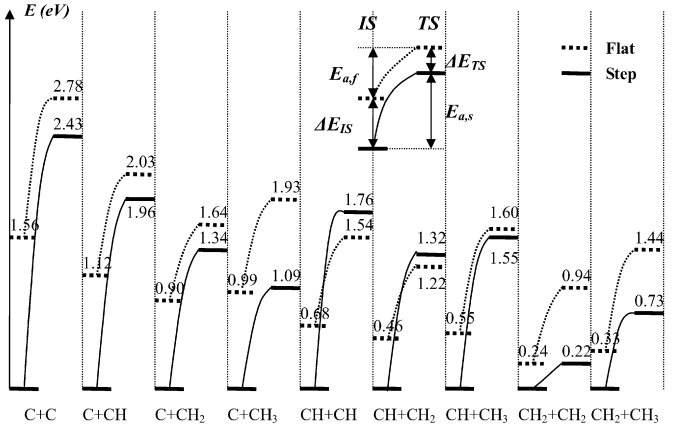

Fig. 4. Energy profiles of all possible $C_1 + C_1$ coupling pathways on both the flat and stepped Co(0001). In each coupling pathway the IS on the step sites is chosen as the zero point.

Table 5
Activation energies (eV) of all possible $C_1 + C_1$ coupling pathways on both the flat and stepped Co(0001)

	C + C	C + CH	C + CH_2	C + CH_3	CH + CH	CH + CH_2	CH + CH_3	CH_2 + CH_2	CH_2 + CH_3
$E_{a,f}$	1.22	0.91	0.74	0.94	0.86	0.76	1.05	0.70	1.11
$E_{a,s}$	2.43	1.96	1.34	1.09	1.76	1.32	1.55	0.22	0.73
ΔE_{IS}	1.56	1.12	0.90	0.99	0.68	0.46	0.55	0.24	0.33
ΔE_{TS}	0.35	0.07	0.30	0.84	−0.22	−0.10	0.05	0.72	0.71

$E_{a,f}$ and $E_{a,s}$ are activation energies on the flat and stepped surfaces, respectively. $\Delta E_{\mathrm{IS}}(\Delta E_{\mathrm{TS}})$ is the difference of IS (TS) between on the flat and stepped surfaces.

coverage on the flat surface should be higher than that on the step sites, considering that the active step sites are covered by surface species, which in turn increases the possibility of coupling reactions on the flat surface. Therefore, one may expect that when the active step sites are not severely blocked, surface reactions may occur mainly on the step sites, taking advantage of lower TS energies. However, when the step sites are heavily blocked, surface species must diffuse to the flat surface to undergo reactions even with higher TS energies.

4.2. Quasi-equilibrium approximation of the hydrogenation steps

In the last section, we considered and compared the $C_1 + C_1$ coupling reaction rates on both the flat and stepped Co surfaces. If the C_1 species coverages are estimated, we can calculate the reaction rates of all of the $C_1 + C_1$ coupling pathways. In this section, we discuss the hydrogenation of the C_1 species to determine the relative coverages of these species.

First, we need to address the dissociative adsorption of H_2. Under experimental conditions, dissociatively adsorbed hydrogen is expected to be in equilibrium with H_2 in the gas phase. Thus we have

$$H_2(g) + 2* \rightleftharpoons 2H(ad)$$

and

$$K^0 = e^{-\Delta G^0/(RT)} = \frac{\theta_H^2}{\frac{P_{H_2}}{P^0}\theta_*^2},$$

where K^0 is the standard equilibrium constant, ΔG^0 is the standard difference of Gibbs free energy, P^0 is the standard pressure, and θ_H and θ_* are the coverages of adsorbed hydrogen and free surface sites, respectively.

According to the experimental results of Bridge et al. [51], the H adsorption energy is about −73 kJ/mol with respect to H_2 in the gas phase, which is very close to our DFT calculations (with zero-point energy considered). Thus, we can estimate that at 500 K, the standard equilibrium constant is about 1. If the hydrogen partial pressure varies in the range 1 to 100 atm, then the value of θ_H/θ_* can be estimated to be between about 1 and 10. We note that according to our calculations, hydrogen adsorption energies are nearly identical on the step sites and on the flat surface; thus, we would expect similar values of θ_H/θ_* on both sites.

The hydrogenation barriers in this work calculated using SIESTA code, listed in Table 6, are very close to those that we reported earlier using CASTEP code [29]. The hydrogenation processes on the flat and stepped surfaces are plotted together in Fig. 5; the figure shows that the energy of TS of the final hydrogenation step is highest on both the flat and stepped surfaces. This indicates that the final step is the slowest of the hydrogenation steps, which is consistent with experimental results [28].

Table 6
Hydrogenation barriers (eV) on the flat and stepped surfaces

Barriers (eV)	C + H		CH + H		CH_2 + H		CH_3 + H
	$E_{a,1}$	$E_{a,-1}$	$E_{a,2}$	$E_{a,-2}$	$E_{a,3}$	$E_{a,-3}$	$E_{a,4}$
Flat	0.83	1.22	0.65	0.29	0.60	0.74	0.96
Step	0.77	0.73	0.80	0.22	0.41	0.65	0.88

$E_{a,1}$ and $E_{a,-1}$ are the barriers of C + H forward and reverse reaction. The others have the similar meanings.

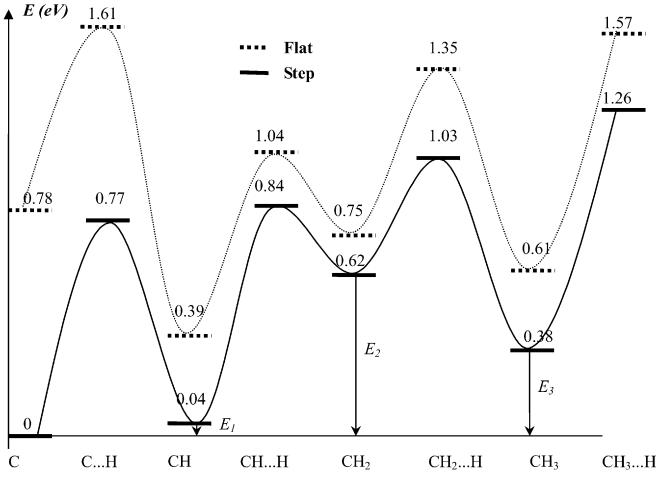

Fig. 5. Energy profiles of carbon hydrogenation on the flat and stepped Co(0001). The IS of $C_{ad} + 4H_{ad}$ on the step sites is chosen as the zero point for both the energy profiles. E_i $(i = 1, 2, 3)$ is the energy difference between adsorbed CH_i and C on the both sites.

It is well known that under FT reaction conditions, methane desorption is irreversible. Therefore, methane formation can be written as

$$C(ad) + H(ad) \underset{k_{-1}}{\overset{k_1}{\rightleftharpoons}} CH(ad) + *, \quad \text{(i)}$$

$$CH(ad) + H(ad) \underset{k_{-2}}{\overset{k_2}{\rightleftharpoons}} CH(ad) + *, \quad \text{(ii)}$$

$$CH_2(ad) + H(ad) \underset{k_{-3}}{\overset{k_3}{\rightleftharpoons}} CH_3(ad) + *, \quad \text{(iii)}$$

$$CH_3(ad) + H(ad) \xrightarrow{k_4} CH_4(g) + *. \quad \text{(iv)}$$

At steady state, we can obtain

$$r_{net} = r_1 - r_{-1} = r_2 - r_{-2} = r_3 - r_{-3} = r_4, \quad (8)$$

$$r_i = k_i \theta_{CH_{i-1}} \theta_H, \quad (9)$$

and

$$r_{-i} = k_{-i} \theta_{CH_i} \theta_*, \quad (10)$$

where r_i (r_{-i}) is the forward (reverse) reaction rate of each hydrogenation step, r_{net} is the net reaction rate, k_i (k_{-i}) is the forward (reverse) reaction rate constant, and θ_{CH_i} is the coverage of surface species CH_i $(i = 0, 1, 2, 3)$.

We first consider the hydrogenation reactions on the step sites. As discussed earlier, the ratio of hydrogen to free site coverage θ_H/θ_* is about 1 to 10 under typical reaction conditions. Combining Eqs. (8)–(10) with the barriers in Table 6, we can have

$$r_{-3} \gg r_4, \quad (11)$$

and thus

$$r_3 \approx r_{-3} \gg r_{\text{net}}. \tag{12}$$

Similarly, we can have

$$r_1 \approx r_{-1} \gg r_{\text{net}} \tag{13}$$

and

$$r_2 \approx r_{-2} \gg r_{\text{net}}. \tag{14}$$

Equations (12)–(14) suggest that hydrogenation reactions (i)–(iii) are in quasi-equilibrium on the step sites. In a similar way, we also can show that the second and third hydrogenation steps are in quasi-equilibrium on the flat surface. However, the first hydrogenation step on the flat surface may not reach quasi-equilibrium because of its high barrier (Fig. 5). On the other hand, the obstacle of forming CH by C hydrogenation on the flat surface can be overcome in another way: CH_2 and CH_3 formed on the step sites can diffuse to the flat surface and decompose to CH there. Through this mechanism, the first hydrogenation step on the flat surface still may be able to reach quasi-equilibrium.

Consequently, the hydrogenation steps on the flat and stepped surfaces can be approximated in quasi-equilibrium under reaction conditions. Thus, the coverages of C, CH, CH_2, and CH_3 on the flat and stepped Co surface have the following relationships:

$$\frac{\theta_{\text{CH}_i}\theta_*^i}{\theta_{\text{C}}\theta_{\text{H}}^i} = e^{-E_i/(RT)} \quad \text{and}$$

$$\theta_{\text{CH}_i} = e^{-E_i/(RT)}\theta_{\text{C}}\frac{\theta_{\text{H}}^i}{\theta_*^i} = e^{-E_i/(RT)}\theta_{\text{C}}t^i, \quad i = 1, 2, 3, \tag{15}$$

where t is equal to $\theta_{\text{H}}/\theta_*$ and E_i is the relative stability of CH_i with respect to the C atom and equal to the energy difference between adsorbed CH_i and C, as shown in Fig. 5. From Eq. (15), we can find that the surface coverages of C_1 species can be evaluated based their thermodynamic stability.

4.3. Comparison among all possible $C_1 + C_1$ coupling pathways

To determine which pathway is responsible for chain propagation in FT synthesis, we need to calculate the reaction rates of all possible $C_1 + C_1$ coupling reactions. According to Eq. (15), the reaction rates of $CH_i + CH_j$ ($i, j = 0, 1, 2, 3$) coupling can be expressed as

$$r_{i,j} = Ae^{-E_a/(RT)}\theta_{\text{CH}_i}\theta_{\text{CH}_j} = Ae^{-(E_a+E_i+E_j)/RT}t^{i+j}\theta_{\text{C}}^2, \tag{16}$$

where E_a is the barrier of $C_1 + C_1$ coupling reactions; A is the pre-exponential factor [52], which may be reasonably assumed to be 10^{13} s^{-1}; and the temperature, T, is chosen to be 500 K.

We first use the calculated data in Table 5 to evaluate the rates of the coupling reactions on the step sites. The results are listed in Table 7. Then, using Eq. (7), we can calculate the coupling reaction rates on the flat surface; these are given in Table 8. Note that in Table 8, θ_{C} is the carbon coverage not on the flat surface, but on the step sites. Also note that the absolute DFT error in this work may be >0.1 eV; however, the relative accuracy may be rather high, because the same code is used for similar reactions on the same surface. Therefore, the comparison among these results in Tables 7 and 8 still may be reliable.

Table 7
Reaction rates (s^{-1}) of all possible $C_1 + C_1$ coupling pathways on the step sites. θ_{C} is the carbon coverage on the step sites and t is equal to $\theta_{\text{H}}/\theta_*$

Pathway	C + C	C + CH	C + CH_2
Reaction rate	$3.3 \times 10^{-12}\theta_{\text{C}}^2$	$7.1 \times 10^{-8}t\theta_{\text{C}}^2$	$1.8 \times 10^{-7}t^2\theta_{\text{C}}^2$
Pathway	C + CH_3	CH + CH	CH + CH_2
Reaction rate	$1.6 \times 10^{-2}t^3\theta_{\text{C}}^2$	$2.9 \times 10^{-6}t^2\theta_{\text{C}}^2$	$1.1 \times 10^{-7}t^3\theta_{\text{C}}^2$
Pathway	CH + CH_3	CH_2 + CH_2	CH_2 + CH_3
Reaction rate	$1.4 \times 10^{-7}t^4\theta_{\text{C}}^2$	$2.0 \times 10^{-2}t^4\theta_{\text{C}}^2$	$3.7 \times 10^{-5}t^5\theta_{\text{C}}^2$

Table 8
Reaction rates (s^{-1}) of all possible $C_1 + C_1$ coupling pathways on the flat surface

Pathway	C + C	C + CH	C + CH_2
Reaction rate	$9.8 \times 10^{-16}s^{-2}\theta_{\text{C}}^2$	$1.4 \times 10^{-8}s^{-2}t\theta_{\text{C}}^2$	$1.7 \times 10^{-10}s^{-2}t^2\theta_{\text{C}}^2$
Pathway	C + CH_3	CH + CH	CH + CH_2
Reaction rate	$3.4 \times 10^{-11}s^{-2}t^3\theta_{\text{C}}^2$	$4.8 \times 10^{-4}s^{-2}t^2\theta_{\text{C}}^2$	$1.1 \times 10^{-6}s^{-2}t^3\theta_{\text{C}}^2$
Pathway	CH + CH_3	CH_2 + CH_2	CH_2 + CH_3
Reaction rate	$4.4 \times 10^{-8}s^{-2}t^4\theta_{\text{C}}^2$	$1.1 \times 10^{-9}s^{-2}t^4\theta_{\text{C}}^2$	$2.6 \times 10^{-12}s^{-2}t^5\theta_{\text{C}}^2$

θ_{C} is the carbon coverage on the step sites, t is equal to $\theta_{\text{H}}/\theta_*$ and s is the ratio of free site coverage on the step sites to that on the flat surface.

From the results in Tables 7 and 8, we can clearly see that C + CH_3 and CH_2 + CH_2 coupling are the most effective chain growth pathways on the step sites, whereas CH + CH coupling is the fastest one on the flat surface. All of the other pathways can be expected to be negligible. On the step sites, C + CH_3 coupling has moderate reactant stability and barrier, giving rise to a good reaction rate; for CH_2 + CH_2 coupling, although the stability of reactant is much worse than other species, the barrier is very low, still resulting in a high reaction rate. On the flat surface, the coupling barriers for all of the coupling pathways (Table 5) do not change much, leading to a high reaction rate for the coupling of the stable CH species (CH + CH). For the traditional mechanism, CH_3 + CH_2, even though the barrier is moderate, the instability of the reactants causes the reaction rate to be three orders smaller than C + CH_3 and CH_2 + CH_2 on the step sites and eight orders smaller than CH + CH on the flat surface.

Which of the three fast pathways is the most efficient on Co? It may depend on the reaction condition. For example, the rates of the C + CH_3 and CH_2 + CH_2 on the step sites are the product of the same concentration term, θ_{C}^2, a similar constant term of $\sim 10^{-2}$, and a ratio of hydrogen to free site coverage, $\theta_{\text{H}}/\theta_*$, with different orders. This suggests that changing H_2 pressure may change the relative rates of the two $C_1 + C_1$ coupling pathways to some extent. Similarly, with increasing CO

pressure, the step sites may become severely blocked, giving rise to smaller s value, which increases the rates of the coupling pathways on the flat surface compared with those on the step sites.

Generally, CO dissociation occurs on the step sites, because the CO dissociation barrier on the flat surface is very high [39]. Because CO can dissociate continually under reaction conditions, it may not be severely blocked on the Co surface. Thus, the two couplings ($C + CH_3$ and $CH_2 + CH_2$) on the step sites would be expected to be more effective than the $CH + CH$ coupling on the flat surface.

There is another argument against the $C + C$ coupling reactions on the flat surface. The rates in Table 8 are calculated based on the assumption that surface species on the stepped and flat surface can reach equilibrium. When considering the relative low mobility of adsorbed C and CH [34], Eq. (7) may not precisely describe the relationship between the reaction rates on the stepped and flat surfaces, especially those involving adsorbed C and CH. Considering that carbon atoms are formed from CO dissociation on the step sites, if equilibrium of the C_1 species is not achieved, then the actual ratios of coverages of the C_1 species on the step sites to those on the flat surface must be higher than those demonstrated in Eqs. (1) and (2). Therefore, the real reaction rates on the flat surface are lower than those estimated by Eq. (7). Consequently, the estimated $C_1 + C_1$ coupling rates on the flat surface in Table 8 are higher than the actual rates, especially for the coupling reactions involved with C and CH. Given these considerations, we suggest that the $C + C$ coupling reactions occur mainly on the step sites. For the same reason, the hydrogenation steps also may occur on step sites.

4.4. General discussion

We have identified the two major chain growth pathways ($CH_3 + C$ and $CH_2 + CH_2$) on Co from DFT calculations and kinetic analysis based on the $C_1 + C_1$ coupling reactions. We also have calculated all of the reactions of $C_2 + C_1$ and $C_3 + C_1$ coupling at step sites (detailed results are presented in our subsequent paper [53]). We found that (i) the results of $C_2 + C_1$ coupling are identical to those of $C_3 + C_1$ coupling, and (ii) the coupling reactions of $RCH_2 + C$ and $RCH + CH_2$ remain the major chain growth pathways. However, we also found that the barriers of $RC + C$ and $RC + CH$ in $C_2 + C_1$ and $C_3 + C_1$ coupling are lower than those in $C_1 + C_1$ coupling; for instance, the barrier of $CH_3C + CH$ is 1.44 eV, which is 0.32 eV lower than that of $CH + CH$. Similarly, the barrier of $CH_3C + C$ is 0.38 eV lower than that of $CH + C$. Consequently, the coupling of $RC + C$ and $RC + CH$ also may contribute to the chain growth in FT synthesis under certain reaction conditions if chain length $n \geqslant 2$. In other words, there may be four possible channels of chain growth on Co when $n \geqslant 2$, as shown in Fig. 6.

Based on the foregoing reasoning, we propose the following scheme for the FT mechanism on Co (Fig. 6): For $C_1 + C_1$ coupling, the $CH_3 + C$ and $CH_2 + CH_2$ coupling on the step sites are the major chain growth mechanisms in FT synthesis. The $CH + CH$ coupling on the flat surface may not be ruled out completely, but may be less important; thus, it is not included in the scheme. If the chain length $n \geqslant 2$, then, in addition to $RCH_2 + C$ and $RCH + CH_2$ coupling, the other two channels ($RC + C$ and $RC + CH$) also may contribute to the chain growth. It should be mentioned that all hydrogenation and dehydrogenation reactions except the final step (alkane desorption) are very fast in FT synthesis. Surface species (e.g., CH_3C and CH_2CH_2 formed from the $CH_3 + C$ and $CH_2 + CH_2$ coupling) can be readily hydrogenated or dehydrogenated to give the initial chains (e.g., CH_3CH_2 and CH_3CH) for the next chain propagation step.

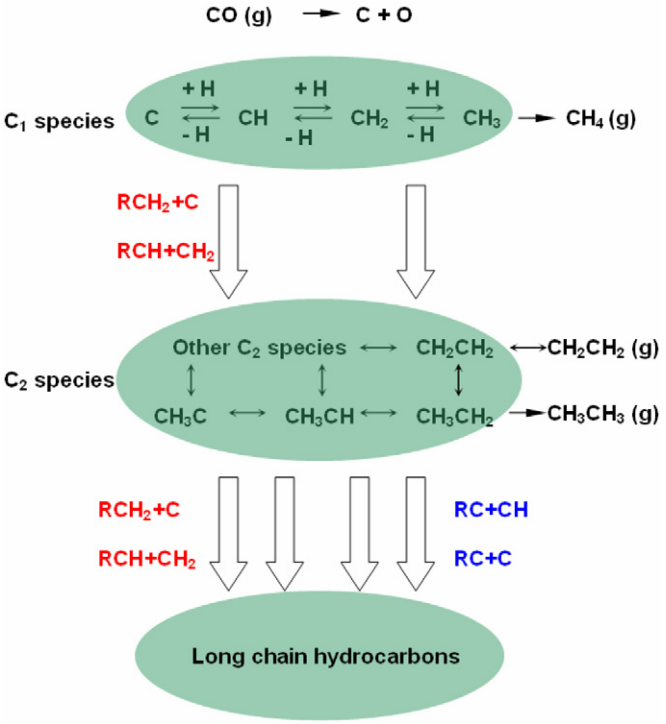

Fig. 6. The mechanism of FT synthesis based on our quantitative analysis. (1) CO and H_2 dissociation. (2) Hydrogenation/dehydrogenation of C_1 species (in quasi-equilibrium) and CH_4 desorption. (3) Two pathways of chain growth, the $CH_3 + C$ and $CH_2 + CH_2$ coupling. (4) Hydrogenation/dehydrogenation of C_2 species, and CH_3CH_3 and CH_2CH_2 desorption. (5) The coupling of $RCH_2 + C$, $RCH + CH_2$, $RC + CH$ and $RC + C$.

Recently, based on the barriers of $C + C$ coupling on Ru(0001) Liu and Hu [31] suggested that the coupling of $C + CR$ that has the lowest barrier might be a major channel for chain growth. Interestingly, this $C + C$ coupling pathway is one of our four channels determined from the Co surfaces, although the result of Liu and Hu was obtained from Ru(0001). It should be stressed that the reaction conditions and different surfaces can change the relative rates of the $C + C$ coupling reactions to some extent.

The mechanism on Co proposed herein is consistent with the experimental work in the literature [21–23]. For example, in the experimental work of Brady and Pettit [21,22], CH_2N_2 decomposed into CH_2 species and N_2 on a range of transition metals. In the absence of H_2, the main product was C_2H_4. This finding indicated that the $CH_2 + CH_2$ coupling is indeed feasible on transition metals, which is consistent with our mechanism. In the presence of H_2, the products were a mixture of

Table 9
Differences between the coadsorption energy of CH_x ($x = 0$–3) and the isolated adsorption energy on the stepped Co surface (coadsorption energy–isolated adsorption energy)

Energy difference (eV)	C	CH	CH_2	CH_3
C	0.21	–	–	–
CH	0.25	0.28	–	–
CH_2	∼0.00	0.14	∼0.00	–
CH_3	∼0.00	0.14	0.16	–

hydrocarbons with a similar distribution to that produced in CO hydrogenation. On the other hand, CH_2 species may be easily hydrogenated into CH_3 species and CH_4 or dehydrogenated to CH and C. Thus, $CH_3 + C$ coupling still may contribute to the chain growth.

We note that although this study aimed to quantitatively determine the chain growth mechanism in FT synthesis, it has not considered the effect of surface coverage on the adsorption energies and reaction barriers. However, we have performed some calculations to shed light on the surface coverage effect on our results. We calculated the coadsorption of CH_x ($x = 0$–3) on the stepped surface in a $p(4 \times 3)$ unit cell. The differences between the coadsorption energy and the isolated adsorption energy, given in Table 9, demonstrate that the differences are reasonably small, suggesting that the surface coverage may not significantly affect our results.

With the foregoing quantitative analysis, we are now in a position to answer the question raised in the Introduction. To determine the mechanism in a catalytic system with a complicated network of reactions, we must (i) obtain the thermodynamic stabilities of all possible intermediates in the network, (ii) determine the barrier of each elementary step, and (iii) estimate the rates of all possible pathways using kinetic analysis. It is noteworthy that these three elements should be considered together; using any one of them in isolation is likely to give misleading results. This obviously is very demanding experimentally. However, with the modern computing power, it can be achieved for most catalytic systems from first-principles calculations.

5. Conclusion

This work represents a quantitative approach to determine the reaction mechanism for a catalytic system with a complicated network of reactions. Having performed extensive DFT calculations to investigate the mechanism of FT synthesis on Co and thoroughly analyzed the calculation results, we now have a deeper understanding of FT synthesis on Co and, consequently, can draw the following conclusions:

1. The ratio of reaction rates between step sites and flat terrace sites is related to the ratio of free site coverage at steps to that on terraces and the difference of TS energies between both sites. It is independent of the ISs. Generally, for surface reactions, steps are favored over terraces.
2. Under FT reaction conditions, surface C_1 species can be approximately considered as in equilibrium at steady state, and a quantitative relationship among these species can be derived [Eq. (15)].
3. $CH_3 + C$ and $CH_2 + CH_2$ coupling at steps are likely to be the major $C_1 + C_1$ coupling pathways in FT synthesis on Co; $CH + CH$ coupling on terraces also may contribute under certain conditions. Calculations of $C_2 + C_1$ and $C_3 + C_1$ coupling suggest that $RCH_2 + C$ and $RCH + CH_2$ are the major $C + C$ coupling pathways and that $RC + C$ and $RC + CH$ also may be of some importance for the chain growth if $n \geqslant 2$. The reaction conditions, such as reactant partial pressure, also may affect the mechanism to some extent.

Acknowledgments

We gratefully thank The Queen's University of Belfast for computing time. J.C. acknowledges Johnson Matthey for financial support.

References

[1] M.E. Dry, Appl. Catal. A 138 (1996) 319.
[2] M.E. Dry, Catal. Today 71 (2002) 227.
[3] H. Schulz, Appl. Catal. A 186 (1999) 3.
[4] J.J.C. Geerlings, J.H. Wilson, G.J. Kramer, H.P.C.E. Kuipers, A. Hoek, H.M. Huisman, Appl. Catal. A 186 (1999) 27.
[5] P. Biloen, W.M.H. Sachtler, Adv. Catal. 30 (1981) 165.
[6] C.K. Rofer-Depoorter, Chem. Rev. 81 (1981) 447.
[7] E. Iglesia, Appl. Catal. A 161 (1997) 59.
[8] R.A. Dictor, A.T. Bell, J. Catal. 97 (1986) 121.
[9] J.G. Ekerdt, A.T. Bell, J. Catal. 62 (1980) 19.
[10] K.R. Krishna, A.T. Bell, J. Catal. 139 (1993) 104.
[11] T. Komaya, A.T. Bell, J. Catal. 146 (1994) 237.
[12] P.M. Maitlis, R. Quyoum, H.C. Long, M.L. Turner, Appl. Catal. A 186 (1999) 363.
[13] M.L. Turner, P.K. Byers, H.C. Long, P.M. Maitlis, J. Am. Chem. Soc. 115 (1993) 4417.
[14] M.L. Tuner, N. Marsih, B.E. Man, R. Quyoum, H.C. Long, P.M. Maitlis, J. Am. Chem. Soc. 124 (2002) 10456.
[15] H.C. Long, M.L. Turner, P. Fornasiero, J. Kašpar, M. Graziani, P.M. Maitlis, J. Catal. 167 (1997) 172.
[16] P.M. Maitlis, J. Mol. Catal. A Chem. 204 (2003) 55.
[17] S.B. Ndlovu, N.S. Phala, M. Hearshaw-Timme, P. Beagly, J.R. Moss, M. Claeys, E. van Steen, Catal. Today 71 (2002) 343.
[18] F. Fischer, H. Tropsch, Brennstoff Chem. 4 (1923) 276;
F. Fischer, H. Tropsch, Brennstoff Chem. 7 (1926) 79;
F. Fischer, H. Tropsch, Chem. Ber. 59 (1926) 830.
[19] H.H. Scorch, N. Goulombic, R.B. Anderson, in: The Fischer–Tropsch and Related Syntheses, Wiley, New York, 1951;
J.F. Kummer, P.H. Emmett, J. Am. Chem. Soc. 75 (1953) 5177.
[20] H. Pichler, H. Schulz, Chem. Ing. Tech. 12 (1970) 1160.
[21] R. Brady, R. Pettit, J. Am. Chem. Soc. 102 (1980) 6181.
[22] R. Brady, R. Pettit, J. Am. Chem. Soc. 103 (1981) 1287.
[23] W.A.A. van Barneveld, V. Ponec, J. Catal. 88 (1984) 382.
[24] M. Araki, V. Ponec, J. Catal. 44 (1976) 439.
[25] P. Biloen, H. Helle, W. Sachtler, J. Catal. 58 (1979) 95.
[26] M. Kaminsky, N. Winograd, G. Geoffroy, M. Vannice, J. Am. Chem. Soc. 108 (1986) 1315.
[27] W. Erley, P. McBreen, H. Ibach, J. Catal. 84 (1983) 229.
[28] J.J.C. Geerlings, M.C. Zonnevylle, C.P.M. de Groot, Surf. Sci. 241 (1991) 302.

[29] X.-Q. Gong, R. Raval, P. Hu, J. Chem. Phys. 122 (2005) 024711.
[30] I.M. Ciobîcă, F. Frechard, A.P.J. Jansen, R.A. van Santen, Stud. Surf. Sci. 133 (2001) 221.
[31] Z.-P. Liu, P. Hu, J. Am. Chem. Soc. 124 (2002) 11568.
[32] I.M. Ciobîcă, F. Frechard, R.A. van Santen, A.W. Kleyn, J. Hafner, Chem. Phys. Lett. 311 (1999) 185.
[33] I.M. Ciobîcă, G.J. Kramer, Q. Ge, M. Neurock, R.A. van Santen, J. Catal. 212 (2002) 136.
[34] I.M. Ciobîcă, The Molecular Basis of the Fischer–Tropsch Reaction, Ph.D. thesis, Technical University of Eindhoven, 2002.
[35] M.C. Wu, D.W. Goodman, J. Am. Chem. Soc. 116 (1994) 1364.
[36] M.C. Wu, D.W. Goodman, Surf. Sci. Lett. 306 (1994) L529.
[37] Q. Ge, M. Neurock, J. Phys. Chem. B 110 (2006) 15368.
[38] M. Mavrikakis, M. Baumer, H.J. Freund, J.K. Norskov, Catal. Lett. 81 (2002) 153.
[39] X.-Q. Gong, R. Raval, P. Hu, Surf. Sci. 562 (2004) 247.
[40] J. Wilson, C. de Groot, J. Phys. Chem. 99 (1995) 7860.
[41] G.A. Beitel, A. Laskov, H. Oosterbeek, E.W. Kuipers, J. Phys. Chem. 100 (1996) 12494.
[42] G.A. Beitel, C.P.M. de Groot, H. Oosterbeek, J.H. Wilson, J. Phys. Chem. B 101 (1997) 4035.
[43] J.M. Soler, E. Artacho, J.D. Gale, A. García, J. Junquera, P. Ordejón, D. Sánchez-Portal, J. Phys. Condens. Matter 14 (2002) 2745.
[44] N. Troullier, J.L. Martins, Phys. Rev. B 43 (1991) 1993.
[45] J.P. Perdew, K. Burke, M. Ernzerhof, Phys. Rev. Lett. 77 (1996) 3865.
[46] C.-J. Chang, P. Hu, J. Am. Chem. Soc. 122 (2000) 2134.
[47] C.-J. Chang, P. Hu, A. Alavi, J. Am. Chem. Soc. 121 (1999) 7931.
[48] A. Alavi, P. Hu, T. Deutsch, P.L. Silvestrelli, J. Hutter, Phys. Rev. Lett. 80 (1998) 3650.
[49] A. Michaelides, P. Hu, J. Am. Chem. Soc. 122 (2000) 9866;
A. Michaelides, P. Hu, J. Chem. Phys. 114 (2001) 2523;
A. Michaelides, P. Hu, J. Chem. Phys. 114 (2001) 5792.
[50] Q. Ge, M. Neurock, H.A. Wright, N.J. Srinivasan, J. Phys. Chem. B 106 (2002) 2826.
[51] M.E. Bridge, C.M. Comrie, R.M. Lambert, J. Catal. 58 (1979) 28;
M.E. Bridge, C.M. Comrie, R.M. Lambert, Surf. Sci. 67 (1977) 393.
[52] M. Boudart, G. Djéga-Mariadassou, in: Kinetics of Heterogeneous Catalytic Reactions, Princeton Univ.;
V.P. Zhdanov, J. Pavlicek, Z. Knor, Catal. Rev. Sci. Eng. 30 (1988) 501.
[53] J. Cheng, P. Hu, P. Ellis, S. French, G. Kelly, C.M. Lok, submitted for publication.